

We are IntechOpen, the world's leading publisher of Open Access books Built by scientists, for scientists

4,400

Open access books available

117,000

International authors and editors

130M

Downloads

Our authors are among the

154

Countries delivered to

TOP 1%

most cited scientists

12.2%

Contributors from top 500 universities



WEB OF SCIENCE™

Selection of our books indexed in the Book Citation Index
in Web of Science™ Core Collection (BKCI)

Interested in publishing with us?
Contact book.department@intechopen.com

Numbers displayed above are based on latest data collected.
For more information visit www.intechopen.com



Reinforcement Fibers in Zinc-Rich Nano Lithium Silicate Anticorrosive Coatings

Carlos Alberto Giudice

UTN (Universidad Tecnológica Nacional),

CIDEPINT (Centro de Investigación y Desarrollo en Tecnología de Pinturas),

La Plata

Argentina

1. Introduction

Well-known the electrochemical nature of most processes of corrosion, the technology of anticorrosive coatings is oriented in the direction of making products that control the development of electrode reactions and that generate the isolating of metal surface by applying films with very low permeability and high adhesion (Sorensen et al., 2011).

The zinc-rich coatings and those modified with extenders and/or metal corrosion inhibitors display higher efficiency than other coatings. A problem that presents this type of primers is the extremely reactive characteristic of metallic zinc; consequently, the manufacturers formulate these coatings in two packages, which imply that the zinc must be incorporated to the vehicle in previous form to coating application (Jianjun et al., 2008 & Lei-lei & De-liang, 2010).

Considering the concept of sacrificial anode (cathodic protection), coatings that consist of high purity zinc dust dispersed in organic and inorganic vehicles have been designed; in these materials, when applied in film form, there are close contacts of the particles among themselves and with the base or metallic substrate to be protected.

The anodic reaction corresponds to the oxidation of zinc particles (loss of electrons) while the cathodic one usually involves oxygen reduction (gain of electrons) on the surface of iron or steel; the “pressure” of electrons released by zinc prevents or controls the oxidation of the metal substrate. Theoretically, the protective mechanism is similar to a continuous layer of zinc applied by galvanizing with some differences because the coating film initially presents in general a considerable porosity (Jegannathan et al., 2006).

In immersion conditions, the time of protection depends on the zinc content in the film and on its dissolution rate. The mechanism is different for films exposed to the atmosphere, because after the cathodic protection in the first stage, the action is restricted substantially to a barrier effect (inhibition resistance) generated by the soluble zinc salts from corrosion by sealing the pores controlling access to water, water vapor and various pollutants. Due to the

above, it is necessary to find the appropriate formulation for each type of exposure in service (Hammouda et al., 2011).

With regard to zinc corrosion products, they are basic compounds whose composition varies according to environmental conditions (Wenrong et al., 2009); they are generally soluble in water and can present amorphous or crystalline structure. In atmospheric exposure, zinc-based coatings that provide amorphous corrosion products are more efficient since these seal better the pores and therefore give a higher barrier effect (lower permeability). Fortunately, zinc-rich coatings of satisfactory efficiency in outdoor exposure display in the most cases amorphous corrosion products.

The durability and protective ability depends, in addition to environmental factors, on the relationship between the permeability of the film during the first stage of exposure and the cathodic protection that takes place (Xiyang et al., 2010). The protection of iron and steel continues with available zinc in the film and effective electrical contact; therefore, particularly in outdoor exposure, the time of satisfactory inhibitory action may be more prolonged due to the polarizing effect of the corrosion products of zinc (Thorslund Pedersen et al., 2009).

A cut or scratch of the film applied on polarized panel allows again the flow of protective electrical current: metallic zinc is oxidized and the film is sealed again. A substantial difference with other types of coatings is that the corrosive phenomenon does not occur under the film adjacent to the cut (undercutting).

With respect to spherical zinc, the transport of current between two adjacent particles is in tangential form and consequently the contact is limited. With the purpose of assuring dense packing and a minimum encapsulation of particles, the pigment volume concentration (PVC) must be as minimum in the order of the critical pigment volume concentration (CPVC).

The problems previously mentioned led to study other shapes and sizes of zinc particles. The physical and chemical properties as well as the behaviour against the corrosion of these primers are remarkably affected by quoted variables and in addition, by the PVC; thus, for example, it is possible to mention the laminar zinc, which was intensely studied by the authors in other manuscripts (Giudice et al., 2009 & Pereyra et al., 2007).

The objective of this paper was study the influence of the content and of the nature of reinforcement fibers as well as the type of inorganic film-forming material, the average diameter of spherical zinc dust and the pigment volume concentration on performance of environmentally friendly, inorganic coatings suitable for the protection of metal substrates. The formulation variables included: (i) two binders, one of them based on a laboratory-prepared nano solution lithium silicate of 7.5/1.0 silica/alkali molar and the other one a pure tetraethyl silicate conformed by 99% w/w monomer with an appropriate hydrolysis degree; (ii) two pigments based on spherical microzinc (D 50/50 4 and 8 μm); (iii) three types of reinforcement fibers used to improve the electric contact between two adjacent spherical zinc particles (graphite and silicon nitride that behave like semiconductor, and quartz that is a non-conductor as reference); (iv) three levels of reinforcement fibers (1.0, 1.5 and 2.0% w/w on coating solids) and finally, (v) six values of pigment volume concentration (from 57.5 to 70.0%).

2. Materials and methods

2.1 Characterization of main components

2.1.1 Film-forming materials

Water-based nano lithium silicate of 7.5/1.0 silica/alkali molar ratio. Previous experiences with these solutions on glass as substrate allowed infer that as silicon dioxide content in the composition increases the film curing velocity also increases and that in addition the dissolution rate decreases.

For this study, a commercial colloidal lithium silicate (3.5/1.0 silica/alkali molar ratio in solution at 25% w/w) was selected; with the aim of increasing the silica/alkali ratio, a 30% w/w colloidal alkaline solution of nanosilica was used (sodium oxide content, 0.32%). The aim was to develop a system consisting of an inorganic matrix (alkaline silicate) and a nanometer component (silica) evenly distributed in that matrix with the objective of determining its behaviour as binder for environment friendly, anticorrosive nano coatings.

Solvent-based, partially hydrolyzed tetraethyl orthosilicate. The tetraethyl orthosilicate is synthesized from silicon tetrachloride and anhydrous ethyl alcohol. This product commercializes as condensed ethyl silicates and usually contains approximately 28% w/w of SiO₂ and at least 90% w/w monomer. The additional purification removes waste products of low boiling point (mainly ethanol) and the dimmers, trimmers, etc.; in some cases, this treatment allows obtaining pure tetraethyl silicate conformed by 99% w/w monomer.

Theoretically, the complete hydrolysis of ethyl silicate generates silica and ethyl alcohol. Nevertheless, the real hydrolysis never produces silica in form of SiO₂ (diverse intermediate species of polysilicates are generated). Through a partial hydrolysis under controlled conditions, it is possible to obtain a stable mixture of polysilicate prepolymers. The stoichiometric equation allows calculating the hydrolysis degree X (Giudice et al., 2007 & Hoshyargar et al., 2009).

The pure or condensed ethyl silicate does not display good properties to form a polymeric material of inorganic nature. In this paper, ethyl silicate was prepared with 80% hydrolysis degree in an acid medium since catalysis carried out in advance in alkaline media led to a fast formation of a gel.

The empirical equation of ethyl silicate hydrolyzed with degree X was used to estimate the weight of the ethyl polysilicate and the hydrolysis degree, through the calculation of the necessary amount of water. The weight was obtained replacing the atomic weights in the mentioned empirical formula; the result indicates that it is equal to 208-148 X.

The percentual concentration of the silicon dioxide in the ethyl polysilicate is equal to the relation molecular weight of SiO₂ x 100 / weight of the ethyl polysilicate; consequently, SiO₂, % = 60 x 100 / (208-148 X). On the other hand, to calculate the water amount for a given weight of tetraethyl orthosilicate and with the purpose of preparing a solution of a predetermined hydrolysis degree, the equation weight of water = 36 (100 X) / 208 was used.

Finally, the amount of isopropyl alcohol necessary to reach the defined percentual level the silica content was calculated. It is possible to mention that after finishing the first hydrolysis

stage of tetraethyl orthosilicate that leads to the silicic acid formation, the absence of alcohol would generate the polycondensation of mentioned acid with silica precipitation and the null capacity to conform a polymeric silicic acid (Wang et al., 2009 & Yang et al., 2008).

In a first stage, the pure tetraethyl silicate and the isopropyl alcohol were mixed under agitation. Later, the water and the hydrochloric acid solution selected as catalyst were added (the final pH of the solution was slightly acid, 0.01% w/v, expressed as hydrochloric acid); agitation continued until the end of the dissipation of heat (exothermic reaction).

The conclusions from the experiences indicate that: an excessive amount of water (higher than calculated) generates a rapid gelling in the package, a high pH leads to a fast silica precipitation that reduces the capacity of formation of an inorganic polymer of elevated molecular weight and, in addition, a large quantity of acid retards the condensing reaction due to the repulsion of protonated hydroxyl groups (Giudice et al., 2007).

2.1.2 Pigmentation

In this study, two samples of commercial spherical zinc dust were used; the D 50/50 average particle diameters were 4 μm (fine) and 8 μm (regular), Figure 1. The main features were respectively 98.1 and 98.3% of total zinc and 94.1 and 94.2% of metal zinc, which means 5.0 and 5.1% of zinc oxide; in addition, metal corrosion inhibitors displayed respectively 2282 and 1162 $\text{cm}^2.\text{g}^{-1}$ values of specific area (BET).

2.1.3 Reinforcement fibers

Nowadays reinforcement fibers are used in many materials to improve their physical and chemical properties (Huang et al., 2009 & Amir et al., 2010). A composite (FRP, fiber-reinforced polymer) is formulated and manufactured with the purpose of obtaining a unique combination of properties; the incorporation of reinforcement fibers to coatings forms a hybrid structure. Fiber is defined as any material that has a minimum ratio of length to average transverse dimension of 10 to 1; in addition, the transverse dimension should not exceed 250 μm .

In anticorrosive coating formulations with hybrid structures, the following reinforcing fibrous materials were used: graphite, silicon nitride and quartz. The levels selected for the experiment were 1.0, 1.5 and 2.0% w/w on coating solids.

Graphite. It is an allotropic form of carbon (hexagonally crystallized). It displays black color with metallic brightness and it is non-magnetic; it has 2.267 $\text{g}.\text{cm}^{-3}$ density at 25 $^{\circ}\text{C}$. Usually, it is used as pigment in coatings to give conductive properties to the film. Graphite is formed by flakes or crystalline plates attached to each other, which are easily exfoliated. The electrons that are between layers are those that conduct electricity, and these are what give the quoted brightness (the light is reflected on the electron cloud) (Yoshida et al., 2009 & Abanilla et al., 2005). In perpendicular direction to the layers, it has a low electrical conductivity, which increases with the temperature (it behaves like a semiconductor); on the other hand, throughout the layers, the conductivity is greater and it is increased with the temperature, behaving like a semi-metallic conductor. In this work, graphite in fiber form was used with average values of 1020 μm and 82 μm for length and transverse dimension, respectively (Figure 2.A).

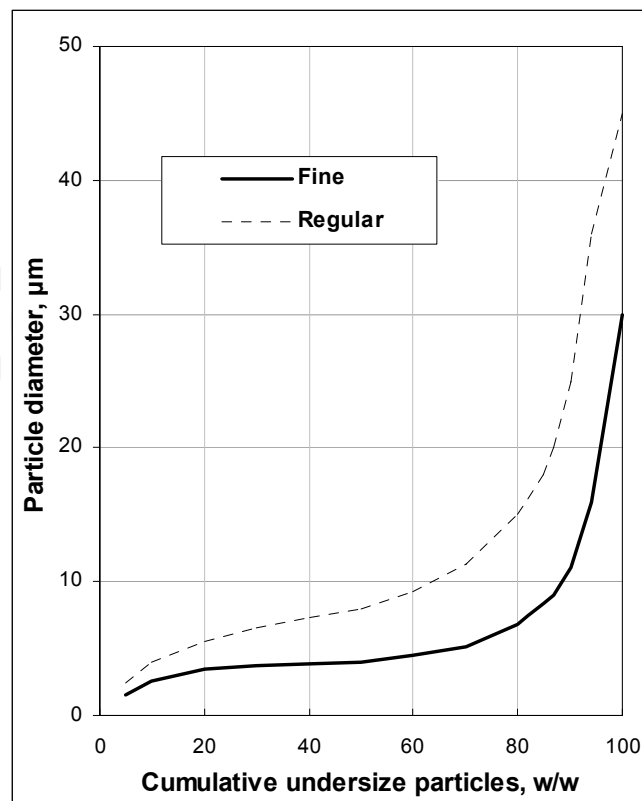


Fig. 1. Commercial spherical zinc dusts. D 50/50 average particle diameters: 4 μm (fine) and 8 μm (regular).

Silicon nitride (Si_3N_4). It displays three different crystal structures (α , β and γ). It is industrially obtained by direct reaction between silicon and nitrogen at temperatures between 1300 and 1400 $^\circ\text{C}$. Silicon nitride is a material frequently used in the manufacture of structural ceramics with high requests of mechanical stress and wear resistance; it displays a moderately high modulus of elasticity and an exceptionally high tensile strength, which makes it attractive for its use in the form of fiber as reinforcement material for coatings films. It behaves like a semiconductor and it has 3.443 $\text{g}\cdot\text{cm}^{-3}$ density at 25 $^\circ\text{C}$. For this experience, hexagonal β phase in the form of fiber has been selected, with average values of 1205 μm and 102 μm for length and transverse dimension, respectively (Figure 2.B).

Quartz. It is rhombohedral crystalline silica reason why it is not susceptible of exfoliation; chemically it is silicon dioxide (SiO_2). Usually it appears colorless (pure), but it can adopt numerous tonalities if it has impurities; its hardness is such that it can scratch the common steels. It is often used in coatings as extender after being crushed and classified by size (average diameter between 1.5 and 9.0 μm). It is an insulating material from the electrical point of view; it has 2.650 $\text{g}\cdot\text{cm}^{-3}$ density at 25 $^\circ\text{C}$ (Chen et al., 2010 & Lekka et al., 2009). In this experience, quartz fibers were used with average values of 1118 μm and 95 μm for length and transverse dimension, respectively (Figure 2.C).

These reinforcements cannot be classified as nano materials since they no have at least one of the dimensions inferior to 100 nm (Aluru et al., 2003; Radhakrishnan et al., 2009; Behler et al., 2009 & Li & Panigrahi 2006).

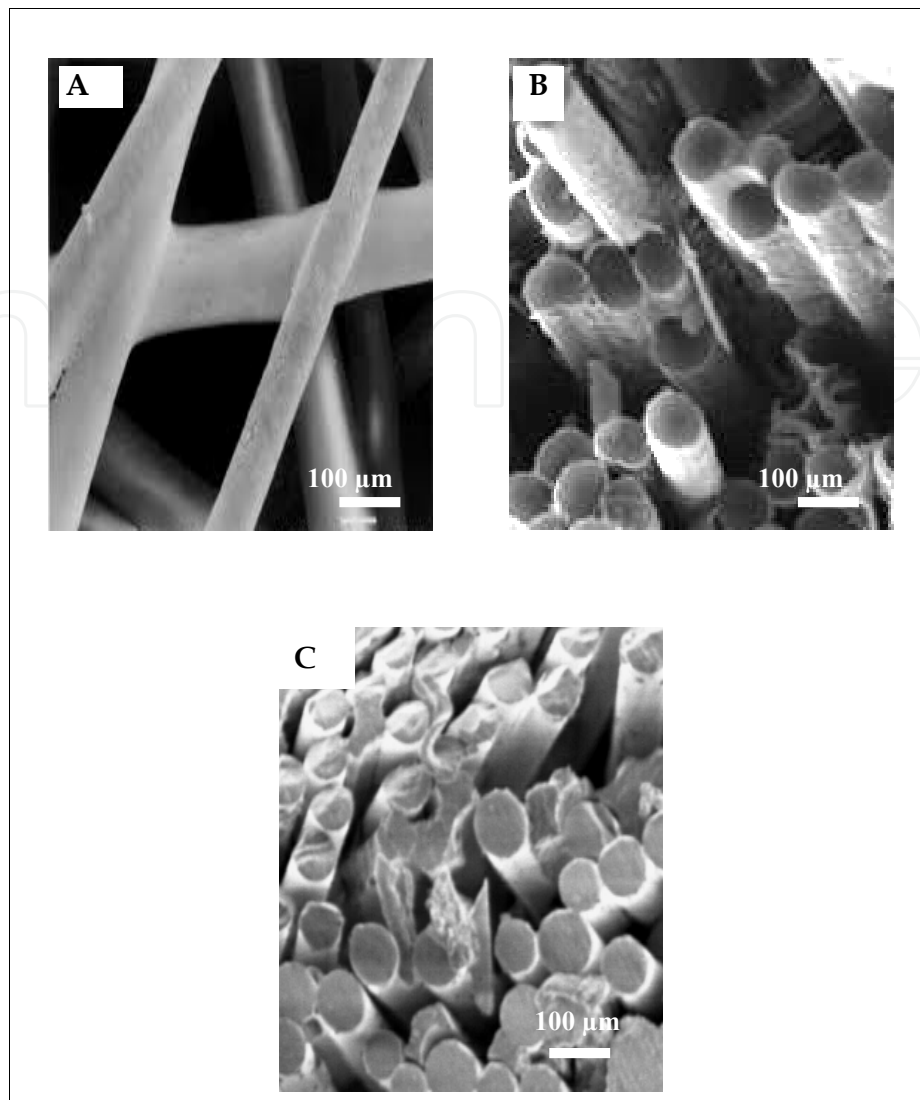


Fig. 2. SEM micrograph of reinforcement fibers: A. Graphite, B. Silicon nitride and C. Quartz.

2.1.4 Rheological agent

Clay modified with amines in gel form was chosen, which was added to the system after finishing the pigment dispersion (1.0% w/w on coating).

2.2 Pigment volume concentration

The physical and mechanical properties of the film and its protective capacity depend on the shape and size of the zinc particles and in addition of the PVC. The critical value (CPVC) is strongly influenced by the ability of binder for wetting the pigment particles.

In this study, PVC values ranged from 57.5 to 70.0%; the variation of two consecutive PVC values was 2.5% in all cases. Preliminary laboratory tests (salt spraying chamber), with values of PVC from 10 to 70% for all formulations, helped to define the range of PVC more convenient to study (Sonawane et al., 2010).

2.3 Manufacture of coatings

In this paper, the manufacture of hybrid coatings was made by ultrasonic dispersion in the vehicle. The efficiency of the fiber dispersion in the polymeric matrix was rheological monitored (viscosity of the system, measured at 10^{-3} sec^{-1} , decreased during the sonification process until reaching a stationary value); the SEM observation corroborated both the efficiency of fiber dispersion and its stability after 3 months in can.

Finally, it should also be mentioned that this type of compositions is provided in two packages with the purpose of avoiding the reaction of metallic zinc with any vestige of moisture in some of the components, which would lead to the formation of gaseous hydrogen. In addition, the system could form a gel because of the reaction between silicic acids and zinc cations. Accordingly, prior to the primer application, the metallic zinc was dispersed for 180 seconds at 1400 rpm in high-speed disperser.

2.4 Preparation of panels

SAE 1010 steel panels were previously degreased with solvent in vapor phase; then they were sandblasted to ASa 2½ grade (SIS Specification 05 59 00/67) obtaining 25 μm maximum roughness R_m . The application was made in a single layer reaching a dry film thickness between 75 and 80 μm . In all cases, and to ensure the film curing before beginning the tests, the specimens were kept in controlled laboratory conditions ($25 \pm 2 \text{ }^\circ\text{C}$ and $65 \pm 5\%$ relative humidity) for seven days.

The study was statistically treated according to the following factorial design: 2 (type of binder) \times 2 (average diameter of spherical microzinc particles) \times 3 (type of reinforcement fibers) \times 3 (level of reinforcement fibers) \times 6 (PVC values), which make 216 combinations. In addition, reference primers (without reinforcement fiber) based on both binders and both spherical microzinc particles for the six mentioned PVC values were also considered, which means in total 24 reference primers. All panels were prepared in duplicate; primer identification is displayed in Table 1.

2.5 Laboratory tests

After curing process, panels of 150 \times 80 \times 2 mm were immersed in 0.1 M sodium chloride solution for 90 days at 25 $^\circ\text{C}$ and pH 7.0. A *visual inspection* was realized throughout the experience; in addition, the *electrode potential* was determined as a function of exposure time; two clear acrylic cylindrical tubes were fixed on each plate (results were averaged).

The tube size was 10 cm long and 5 cm diameter, with the lower edge flattened; the geometric area of the cell was 20 cm^2 . A graphite rod axially placed into the tubes and a saturated calomel electrode (SCE) were selected respectively as auxiliary and reference electrodes. The potential was measured with a digital electrometer of high input impedance.

Similar panels were tested in salt spraying (fog) chamber (1500 hours) under the operating conditions specified in ASTM B 117. After finishing the tests, the panels were evaluated according to ASTM D 1654 (Method A, in X-cut and Method B, in the rest of the surface) to establish the *degree of rusting*.

Film-forming material	(A) Water-based nano lithium silicate of 7.5/1.0 silica/alkali molar ratio
	(B) Solvent-based, partially hydrolyzed tetraethyl orthosilicate
Spherical microzinc	(I) Spherical microzinc (fine), D 50/50 4 μm
	(II) Spherical microzinc (regular), D 50/50 8 μm
Reinforcement fibers	Types: (1) Without, (2) Graphite, (3) Silicon nitride (4) Quartz
	Level: (a) 1.0, (b) 1.5 and (c) 2.0% w/w on coating solids
PVC	Values: 57.5, 60.0, 62.5, 65.0, 67.5 and 70.0%

Table 1. Primer identification.

3. Result and discussion

3.1 Visual observation

Immersion test in 0.1 M sodium chloride solution allowed to observe, particularly in those panels with X-cut, that coatings based on nano-structured film-forming material as binder showed greater amount of white products from corrosion of metallic zinc than in those panels protected with primers made with partially hydrolyzed ethyl silicate as binder. This performance would be supported in the less zinc dispersion ability that displays the first binder, which would generate films more porous.

On the other hand, primers that included fine zinc particles (4 μm) also showed a galvanic activity more important than those made from regular zinc particles (8 μm). A similar conclusion was reached with the primers based on microzinc/conducting reinforcement fibers (graphite and silicon nitride) with respect to those based just on spherical microzinc dusts and mixture with insulating reinforcement fiber (quartz). In turn, it was also observed a rise of the galvanic activity of metallic zinc when the amount of conducting fibers was increasing in the film.

For the lower values of PVC studied, the incorporation of conductive reinforcing fibers in increasing levels led to primers with a galvanic activity also increasing (similar amount of white salts than in primers formulated with PVC nearest to CPVC).

3.2 Corrosion potential

Immediately after finishing the immersion of all coated panels in the electrolyte, the potential was inferior to -1.10 V, a value located in the range of protection of the electrode. It is worth mentioning that cathodic protection is considered finished when the corrosion potential of coated panel increased to more positive values (anodic ones) than -0.86 V (referring to SCE) since the characteristic corrosion points of the iron oxides were visually observed.

The electrode potential measurements as a function of immersion time indicates that both types of binders had a significant influence on the electrode potential: in general, more negative values were obtained with nano-structured film-forming materials, which means that the primers based on lithium silicate showed better cathodic protection than those manufactured with ethyl silicate.

On the other hand, slight differences in electrode potential could also be attributed to the average diameter of zinc particles; it was observed greater galvanic activity in samples prepared with 4 μm than with 8 μm (values more negative of electrode potentials for the former than for the latter).

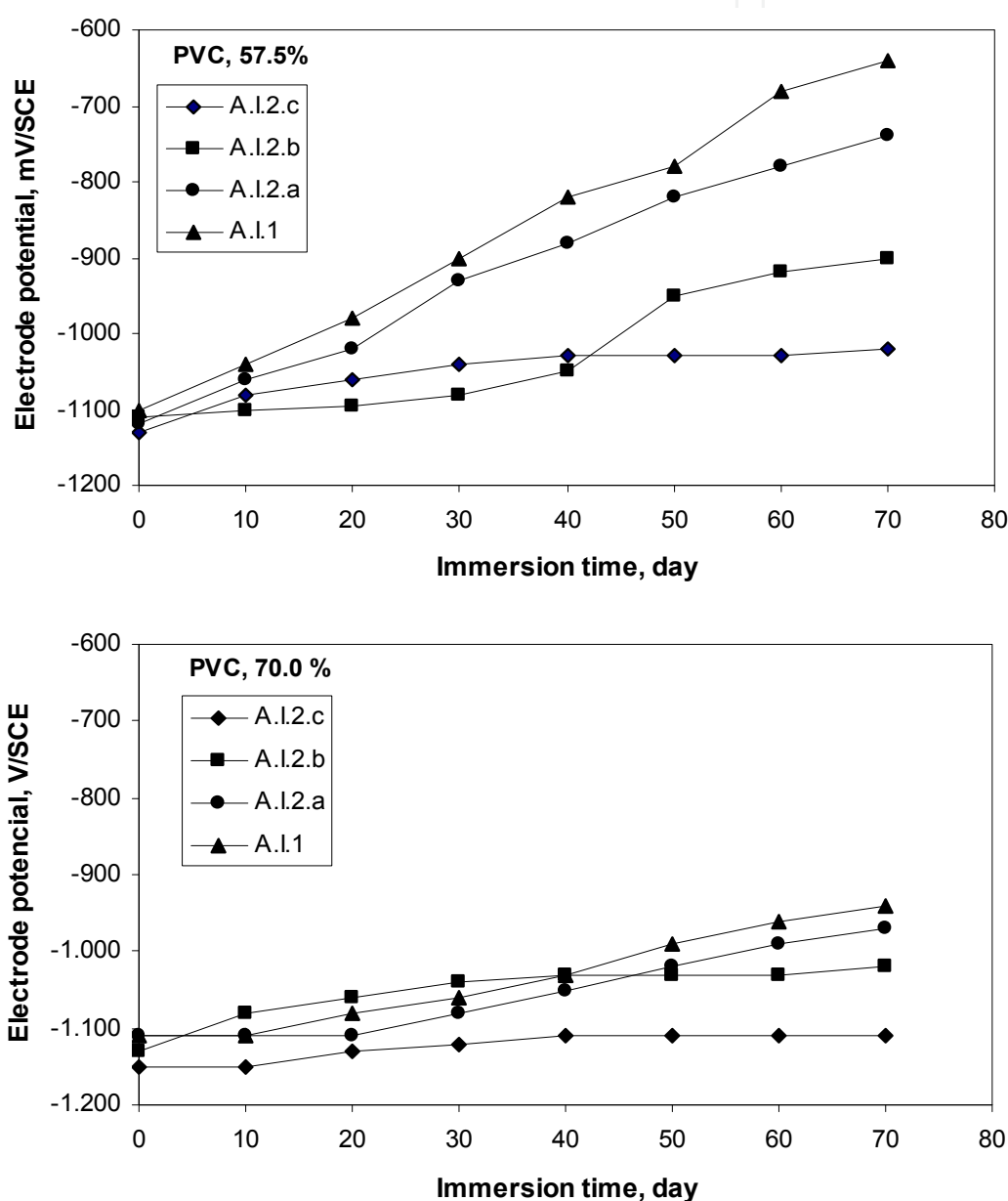


Fig. 3. Electrode potential vs. immersion time in 0.1 M sodium chloride solution at pH 7.0 and 25 °C for primers based on 7.5/1.0 nanosilica/lithium oxide molar ratio, fine microzinc and graphite fibers.

The experimental values indicate a significant shift towards more positive values of potential in those primers with decreasing amounts of conducting reinforcement fibers in their composition (2.0, 1.5 and 1.0% w/w ratio, in that order).

Considering the performance, the worst primers have been formulated both with microzinc dusts alone and mixed with insulation reinforcement fibers.

Finally, there was observed only a slightly decreasing efficiency to the lower values of PVC studied with the incorporation of conductive reinforcing fibers in increasing levels.

Figure 3 includes values of potential versus immersion time in 0.1 M sodium chloride solution at pH 7.0 and 25 °C for primers formulated with 57.5 and 70.0% PVC values and based on 7.5/1.0 nano silica/lithium oxide molar ratio as film-forming material, fine microzinc (D 50/50 4 µm) as pigment inhibiting and graphite as reinforcement fiber in the three levels studied. In addition, this figure displays the corresponding reference primers.

There is a total correlation between conclusions of visual observation and results of the electrode potentials obtained during immersion in 0.1 M sodium chloride solution; therefore, the basis of the quantitative results of electrode potentials are the same that those spelled out in the visual observation.

3.3 Degree of rusting

The performance of panels tested during 1500 hours in salt spraying (fog) chamber (35±1 °C; pH 6.5-7.2; continuous spraying of 5±1% w/w of NaCl solution) are shown in Figure 4 and Figure 5. They include only the average values of the tests performed in the failure in X-cut (Method A) and over the general area of panel (Method B).

The results of Method A were evaluated according to the advance from the cutting area: the value 10 defines a failure of 0 mm while zero corresponds to 16 mm or more. Those results corresponding to Method B were measured taking into account the percentage of area corroded by the environment: the scale ranges from 10 to 0, which means respectively no failure and over 75% of the rusted area.

On the other hand, Figure 6 displays one of the primer with best performance in salt spraying (fog) chamber for 1500 hours: A.I.2.c; applying the Method A, this primer showed a degree of rusting 10 (no failure, which means 0 mm of advance from the cutting area).

To study the variables considered (main effects), a statistical interpretation was carried out. First, the variance was calculated and later the Fisher F test was done.

The results indicated that type of binder, average diameter of microzinc particles, type of reinforcement fibers, level of reinforcement fibers and finally PVC values displayed an important influence on the performance of the protective coatings.

According to results, it was considered desirable for the statistical analysis to take into account all values of PVC studied for allowing a certain margin of safety in the performance since it is possible the generation of heterogeneities in primer composition attributable to poor incorporation of metallic zinc and/or sedimentation in container before applying.

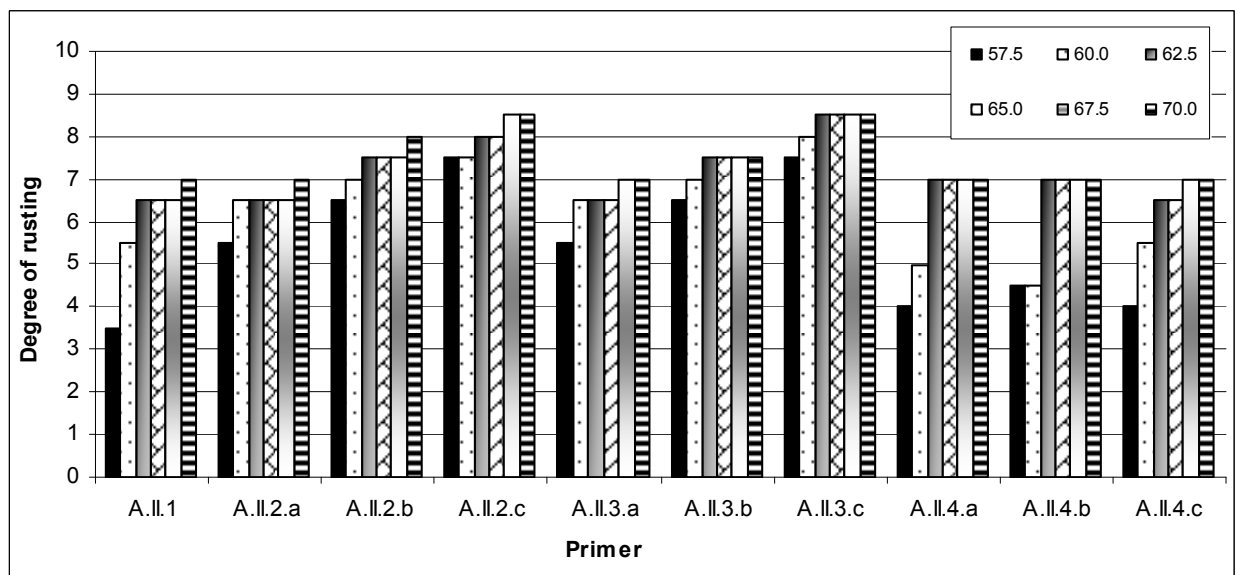
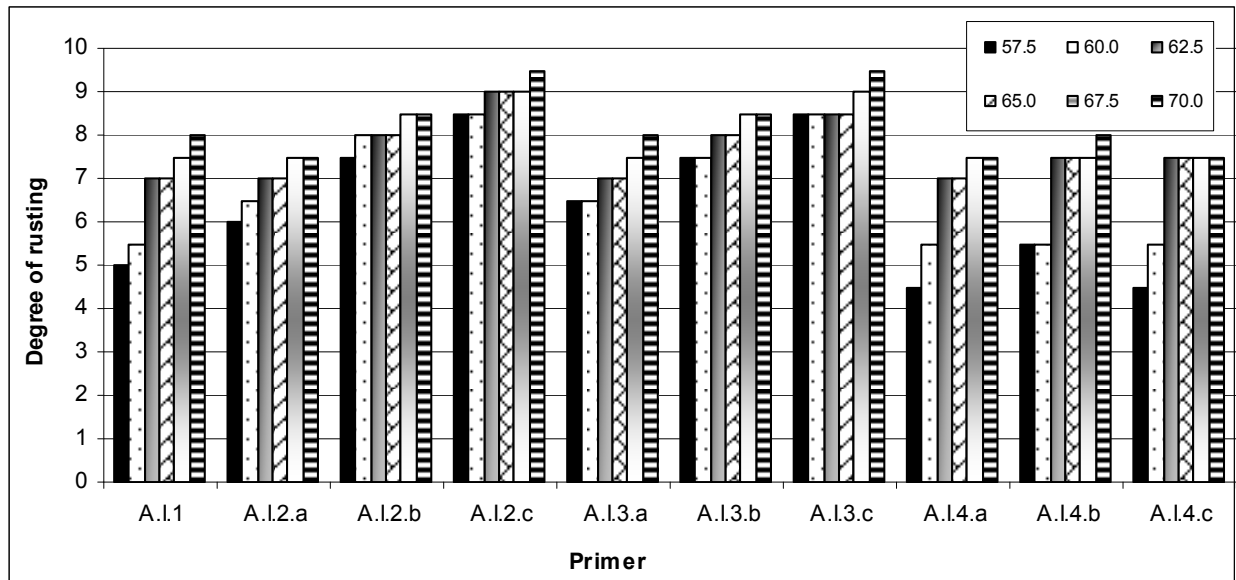


Fig. 4. Coatings based on binder A: Degree of rusting in salt spraying (fog) chamber; average values of failures in X-cut and in general area of panel.

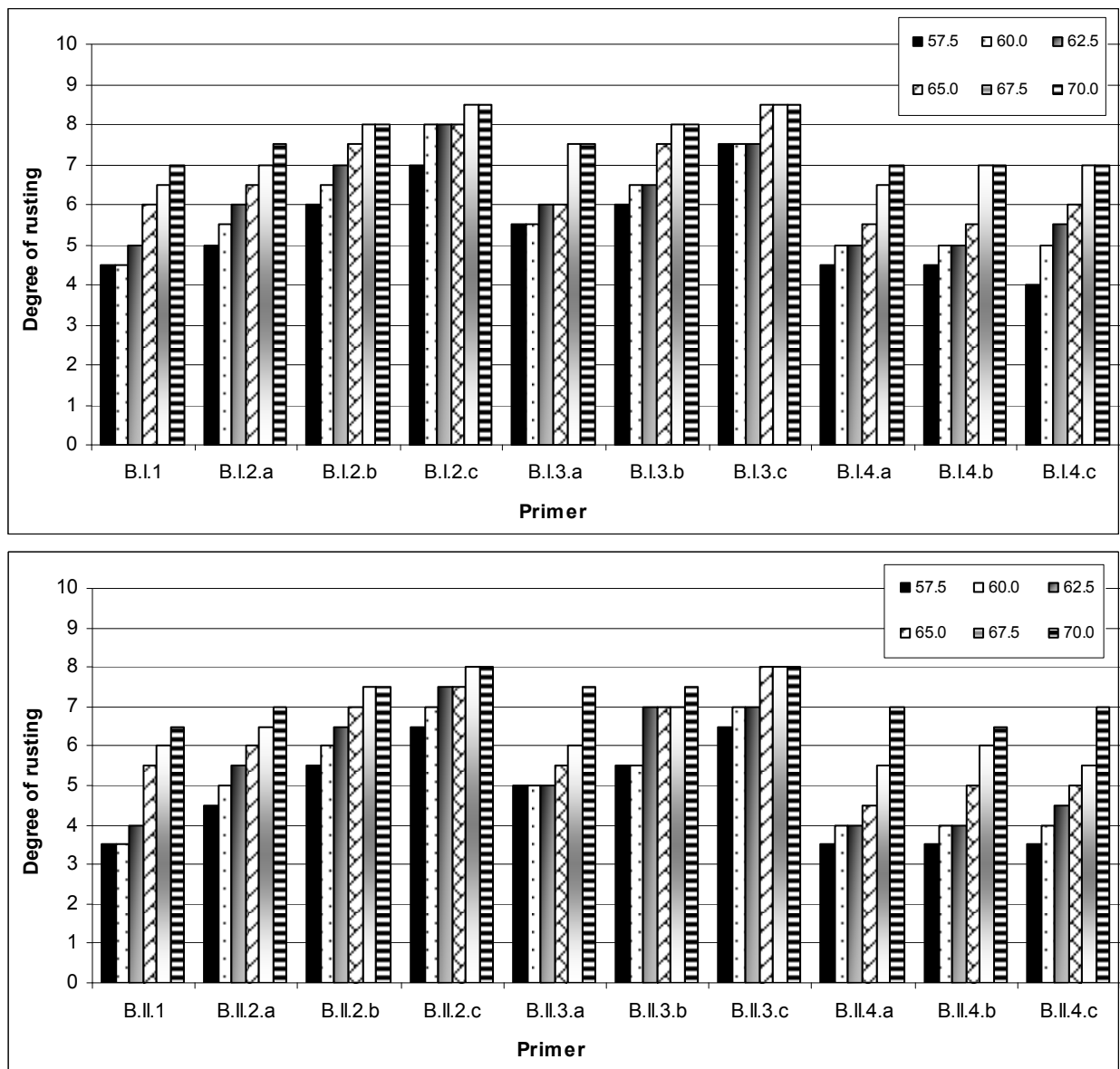


Fig. 5. Coatings based on binder B: Degree of rusting in salt spraying (fog) chamber; average values of failures in X-cut and in general area of panel.

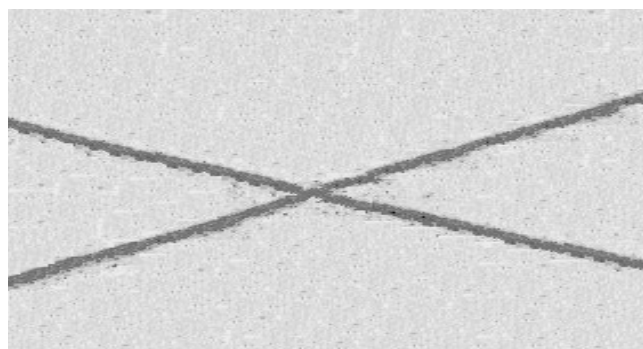


Fig. 6. Primer A.I.2.c, performance in salt spraying (fog) chamber, Method A, degree of rusting: 10.

With the purpose of establishing the efficiency of each protective coating from an anticorrosive point of view, the average value of degree of rusting was calculated for areas with and without cutting. The results of Table 2 confirm the superior performance of water-based nano lithium silicate of 7.5/1.0 silica/alkali molar ratio in relation to solvent-based, partially hydrolyzed tetraethyl orthosilicate, the major efficiency of fine microzinc compared to regular one and the increasing efficiency of primers as the level of conducting reinforcement fibers increased (Ahmed et al., 2010). On this last variable of formulation, it is worth mentioning that primers with 2.0% conducting reinforcement fibers showed the best protective capacity, which would occur due to the improved electric contact between zinc particles and with metallic substrate. On the other hand, the quartz used as reinforcement fiber due to characteristic non-conductive showed a similar performance that the corresponding reference primer (without reinforcement fiber).

Nature of effect	Type of effect	Degree of rusting
		Average values of failures in X-cut and in general area of panel
Type of binder	A	7.1
	B	6.2
Microzinc D 50/50	I	7.0
	II	6.3
Type of reinforcement fibers	1	5.8
	2	7.2
	3	7.2
	4	5.8
Level of reinforcement fibers	a	6.2
	b	6.8
	c	7.3

Table 2. Average values of the simultaneous statistical treatment of all variables.

On the other hand, Table 3 lists the average values and the standard deviations of statistical processing for each primer; in addition, it also displays the general average values for each type of reinforcement fiber taking into account both binders considered. In this table, the highest value also indicates the best performance in terms of the ability to control the metal corrosion. The analysis of the results obtained by using both types of binder displays that the primers based just on two spherical microzinc (reference primers) and non-conducting reinforcement fibers (quartz) in the three considered levels, formulated with reduced values of PVC, showed a sharp decline in corrosion performance. On the other hand, those that included conducting reinforcement fibers (graphite and silicon nitride), despite having been manufactured with a significantly lower level of pigmentation, maintained their efficiency. Corresponding standard deviation values support this conclusion.

These results would be based on the reduced electrical contact between particles of both types of microzinc and the metal substrate, regardless of the corrosion products could not only increase the electrical resistance of the film but also could decrease the amount of available zinc.

The incorporation of conducting reinforcement fibers seems to have favored the conductivity, which leads to reduction of the efficient PVC, according to the abundant amount of zinc corrosion products visually observed, the results of the electrode potentials and those obtained in the salt spraying (fog) chamber. Figures 7 and 8 display the primer films based on binder A (water-based nano lithium silicate of 7.5/1.0 silica/alkali molar ratio), microzinc I (fine, 4 μm) and fiber 2 (graphite) in level c (2.0% w/w) for 57.5% and 70.0% PVC values respectively, after finishing the accelerated aging test. The analysis of the cited figures reveals that despite having larger distance between the particles of microzinc in the case of 57.5% PVC compared with that formulated with 70.0% PVC, the galvanic activity in the two primers is significant in both cases (as evidenced by the amount of white zinc salts). In addition, results of figures show that the conductive reinforcement fibers linked electrically the microzinc particles each other, even in the primer of less PVC (all particles, despite having no direct contact between them, demonstrated activity like sacrificial anodes).

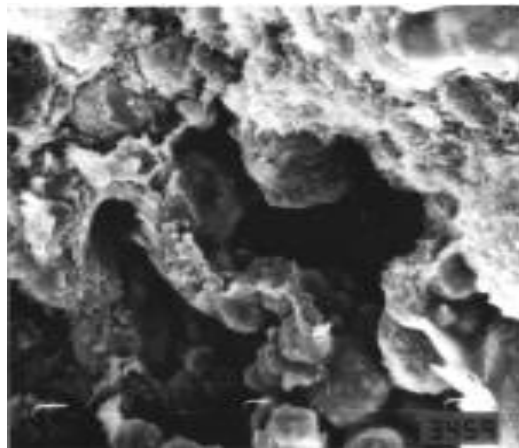


Fig. 7. SEM micrograph of primer A.I.2.c formulated with 57.5% PVC.

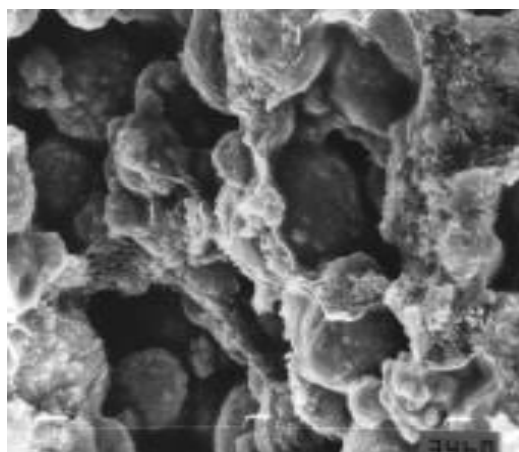


Fig. 8. SEM micrograph of primer A.I.2.c formulated with 70.0% PVC.

Primer	Average values	Standard deviation σ_{n-1}	General average values	Primer	Average value	Standard deviation σ_{n-1}	General average value
A.I.1	6.6	1.16	6.6	B.I.1	5.6	1.07	5.6
A.I.2.a	6.9	0.58	8.0	B.I.2.a	6.2	0.94	7.1
A.I.2.b	8.2	0.41		B.I.2.b	7.2	0.82	
A.I.2.c	8.9	0.38		B.I.2.c	8.0	0.55	
A.I.3.a	7.0	0.63	7.9	B.I.3.a	6.3	0.93	7.1
A.I.3.b	8.0	0.44		B.I.3.b	7.1	0.86	
A.I.3.c	8.8	0.42		B.I.3.c	8.0	0.55	
A.I.4.a	6.4	1.20	6.5	B.I.4.a	5.6	0.97	5.7
A.I.4.b	6.7	1.13		B.I.4.b	5.7	1.08	
A.I.4.c	6.4	1.28		B.I.4.c	5.8	1.17	
A.II.1	6.0	1.34	6.0	B.II.1	4.8	1.33	4.8
A.II.2.a	6.5	0.55	7.2	B.II.2.a	5.8	0.93	6.6
A.II.2.b	7.3	0.52		B.II.2.b	6.7	0.82	
A.II.2.c	7.8	0.49		B.II.2.c	7.4	0.53	
A.II.3.a	6.5	0.55	7.3	B.II.3.a	5.7	0.98	6.6
A.II.3.b	7.2	0.42		B.II.3.b	6.6	0.86	
A.II.3.c	8.2	0.41		B.II.3.c	7.2	0.66	
A.II.4.a	6.1	1.28	6.1	B.II.4.a	4.8	1.29	4.8
A.II.4.b	6.1	1.24		B.II.4.b	4.8	1.21	
A.II.4.c	6.1	1.16		B.II.4.c	4.9	1.24	

Table 3. Average values and standard deviation.

4. Final considerations

To explain the great tendency of zinc particles to corrode at the film surface of water-based nano lithium silicate primers as comparing with those solvent-based, partially hydrolyzed tetraethyl orthosilicate, it is necessary to consider that the first ones are based on binders, as mentioned, with a higher superficial tension. The last one implies inferior wetting, that means lower adhesion, penetration and spreading during metal zinc incorporation previous to application; consequently, they wet with more difficult the zinc particles while the second ones do it in a better way (more reduced interfacial tension).

The above-mentioned characteristic explains the great porosity of zinc-rich nano lithium silicate films and their high cathodic protective activity as comparing with zinc-rich tetraethyl orthosilicate films.

With regard to average diameter of zinc particle, size diminution increases significantly the surface area for a given weight. Since all surfaces have a given level of free energy, the ratio of surface energy to mass in small particles is so great that the particles adhered strongly themselves. For this reason, a lower particle size in a poor dispersion originates a greater flocculates (a high number of unitary particles are associated), which lead to zinc-rich

primer films of high porosity and because of good cathodic protective activity. Moreover, a lower particle size could lead to films with a higher electrical contact (better packaging ability); since the current density is inherent to the chemical nature of zinc dust and the operating conditions of the corrosion cell, the increase in specific area elevates not only the current of protection but also generates a better superficial distribution (more efficient primers). During immersion test in 0.1 M sodium chloride solution, visual inspection of plates protective with zinc-rich primers (both types of binders) showed a more localized steel attack when zinc dust of the higher particle size was used.

Concerning incorporation of reinforcement fibers, the conductive or non-conductive characteristic was a very important variable. The first ones improved notably the primer performance since they increased the electrical contact between particles and with the metallic substrate, particularly in the higher levels in the formulations; the performance is correlated with the higher useful zinc in the film. On the other hand, non-conductive reinforcement fibers did not modify the primer efficiency as compared with reference panels (without reinforcement fibers) and for this reason their incorporation is not justified from technical and economical viewpoints.

Referring to PVC values (zinc content in dry film), previous results of laboratory tests demonstrated that a higher amount of microzinc leads to a longer useful life of primers. Nevertheless, it is important to mention that the choice of zinc content must be made by considering the physical characteristic of the primer film required for each particular case. When pigment volume concentration exceeds largely the CPVC, film properties such as adhesion, flexibility, abrasion resistance, etc. are drastically reduced while when the percentual level is slight under the critical value the efficiency is also considerably diminished.

In the case of primers, which have got incorporated conductive reinforcing fibers, results allow concluding that it is possible to reduce appreciably the PVC without affecting significantly the efficiency in service. In addition, it is important to mention that the quoted diminution of zinc content in the film is direct proportional to decrease the primer cost since it is the most expensive component of the composition.

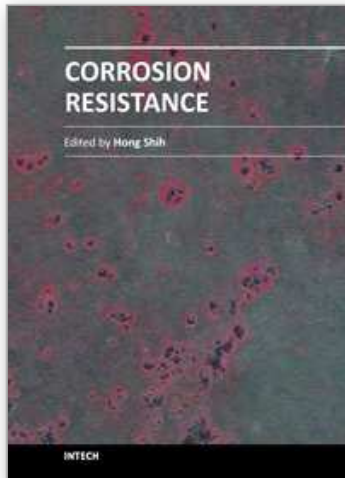
5. References

- Abanilla, M.A.; Li, Y. and Karbhari, V.M. (2005). Durability characterization of wet layup graphite/epoxy composites used in external strengthening, *Composites Part B: Engineering*, Vol. 37, No. 2-3, (August 2005), pp. 200-212, DOI: 10.1016/j.compositesb.2005.05.016
- Ahmed Al-Dulaimi, Ahmed (2010). *Evaluation of polyaniline composites and nanostructures as anti-corrosive pigments for carbon steel*. Masters thesis, Universiti Teknologi Malaysia, Faculty of Chemical and Natural Resource Engineering.
- Aluru, N. et al., in: Gooddard, Brenner, Lyshevski, Iafrate Ed., (2003). *Nanostructure Studies of the Si-SiO₂ Interface*, Handbook of Nanoscience, Engineering and Technology, CRC Press., Washington D.C., USA, 2003, Chapter 11.2.
- Amir, N.; Ahmad, F. and Megat-Yusoff, P. (2010). *Study on Fiber Reinforced Epoxy-based Intumescent Coating Formulations and Their Characteristics*. International Conference on Plant Equipment and Reliability (ICPER 2010), Kuala Lumpur, Malaysia, June 2010.

- Behler, D.K.; Stravato, A.; Mochalin, V.; Korneva, G.; Yushin, G. and Gogotsi, Y. (2009). Nanodiamond-Polymer Composite Fibers and Coatings, *ACS Nano*, 2009, Vol. 3, No. 2, pp 363–369, DOI: 10.1021/nn800445z
- Chen, Y. H.; Yu Chu, J. and Zhu, Q.J. (2010). Effects of Coating on Interfacial Fatigue of Fiber-Reinforced Composites, *Advanced Materials Research, Manufacturing Science and Engineering I*, Vol. 97, No. 101, (March 2010), pp. 830-833, DOI: 10.4028/www.scientific.net/AMR.97-101.830
- Giudice, C.A. and Pereyra, A.M. (2007). Soluble metallic silicates in the anticorrosive inorganic coating formulation with non-flammable properties. *Pittura e Vernici European Coatings*, Vol. 83, No. 7, pp. 48-57, ISSN 0048-4245
- Giudice, C.A. and Pereyra, A.M. (2009). *Tecnología de pinturas y recubrimientos. Componentes, formulación, manufactura y control de calidad*, Ed. edUTecNe, Argentina, 2009, pp. 1-444.
- Hammouda, N.; Chadli, H.; Guillemot, G. and Belmokre, K. (2011). The Corrosion Protection Behaviour of Zinc Rich Epoxy Paint in 3% NaCl Solution, *ACES*, Vol.1 No.2, (April 2011), pp.51-60, DOI: 10.4236/aces.2011.12009
- Hoshyargar, F.; Ali Sherafati, S. and Hashemi, M. (2009). Short communication: A new study on binder performance and formulation modification of anti-corrosive primer based on ethyl silicate resin. *Progress in Organic Coatings*, Vol. 65, No. 3, (July 2009), pp. 410-413, DOI: 10.1016/j.porgcoat.2009.02.006
- Huang, K.M.; Weng, C.J.; Lin, S.Y; Yu, Y.H. and Yeh, J.M. (2009). Preparation and anticorrosive properties of hybrid coatings based on epoxy-silica hybrid materials, *Journal of Applied Polymer Science*, Vol. 112, No. 4, (May 2009), pp. 1933–1942, DOI: 10.1002/app.29302
- Jegannathan, S.; Sankara Narayanan, T.; Ravichandran, K.; and Rajeswari, S. (2006). Formation of zinc phosphate coating by anodic electrochemical treatment. *Surface and Coatings Technology*, Vol. 200, No. 20-21, (May 2006), pp. 6014-6021, DOI: 10.1016/j.surfcoat.2005.09.017
- Jianjun, Y.; Zhenhua, S.; Xiangsheng, M. and Wenlong, L., Deqiang, J. (2008). Corrosion Protective Performance of Coatings. Study on Zinc Ingredient in Zinc Rich Epoxy Primers. *Paint & Coatings Industry*, Vol. 08-2008, (August 2008), DOI: CNKI:SUN:TLGY.0.2008-08-003.
- Lei-lei, M. and De-liang, L. (2010). The Classification and Testing Standards of Zinc Rich Coatings, *Shanghai Coatings*, Vol. 05, (May 2010), DOI: CNKI:SUN:SHTL.0.2010-05-015
- Lekka, M.; Koumoulis, D.; Kouloumbi, N. and Bonora N.P. (2009). Mechanical and anticorrosive properties of copper matrix micro- and nano-composite coatings. *Electrochimica Acta*, Vol. 54, No. 9, (March 2009), pp. 2540-2546, DOI: 10.1016/j.electacta.2008.04.060
- Li, X.; Tabil, L.G. and Panigrahi, S. (2006). Chemical Treatments of Natural Fiber for Use in Natural Fiber-Reinforced Composites: A Review. *Chemistry and Materials Science, Journal of Polymers and the Environment*, Vol. 15, No. 1, (March 2006) pp. 25-33, DOI: 10.1007/s10924-006-0042-3
- Pereyra, A.M. and Giudice, C.A. (2007). Shaped for performance: the combination of lamellar zinc and mica improves the efficiency of zinc-rich primers. *European Coatings Journal*, Vol. 9, pp. 40-45, ISSN 0930-3847

- Radhakrishnan, S.; Siju, C.R.; Mahanta, D.; Patil, S. and Madras, S. (2009). Conducting polyaniline-nano-TiO₂ composites for smart corrosion resistant coatings, *Electrochimica Acta*, Vol. 54, No. 4, (January 2009), pp. 1249-1254 DOI: 10.1016/j.electacta.2008.08.069
- Sonawane, S.; Teo, B.; Brotchie, A.; Grieser, F. and Ashokkumar, M. (2010). Sonochemical Synthesis of ZnO Encapsulated Functional Nanolatex and its Anticorrosive Performance, *Ind. Eng. Chem. Res.*, (January 2010), Vol. 49, No. 5, pp. 2200-2205. DOI: 10.1021/ie9015039
- Sorensen, P.A.; Kiil, S.; Dam-Johansen, K. and Weinell C.E. (2011). Anticorrosive coatings: a review, *Chemistry and Materials Science, Journal of Coatings Technology and Research*, Vol. 6, No. 2, pp. 135-176, DOI: 10.1007/s11998-008-9144-2
- Thorslund Pedersen, L.; Weinell, C.; Hempel, A. S; Verbiest, P; Van Den Bosch, J. and Umicore J. (2009). *Advancements in high performance zinc epoxy coatings Zinc*, Chemicals Source Corrosion 2009, (March 2009), Copyright NACE International
- Wang, D. and Bierwagen, G. (2009). Sol-gel coatings on metals for corrosion protection. *Progress in Organic Coatings*, Vol. 64, No. 4 (March 2009), pp. 327-338. DOI: 10.1016/j.porgcoat.2008.08.010
- Wenrong, J. (2009). The Research Progress on Green Coatings, *Guangdong Chemical Industry*, Vol. 5, (May 2009), DOI: CNKI:SUN:GDHG.0.2009-05-035
- Xiyan, L.; Jianming, J.; Sibon, K. and Jing, Z. (2010) Preparation of Flexible Epoxy Anticorrosive Coatings, *China Coatings*, Vol. 7, (July 2010), DOI: CNKI:SUN:ZGTU.0.2010-07-018
- Yang, F.; Zhang, X.; Han, J. and Du, S. (2008). Characterization of hot-pressed short carbon fiber reinforced ZrB₂-SiC ultra-high temperature ceramic composites, *Journal of Alloys and Compounds*, Vol. 472, No. 1-2, (20 March 2009), pp. 395-399, DOI: 10.1016/j.jallcom.2008.04.092
- Yoshida, K.; Matsukawa, K.; Imai, M. and Yano, T. (2009). Formation of carbon coating on SiC fiber for two-dimensional SiCf/SiC composites by electrophoretic deposition, *Materials Science and Engineering: B*, Vol. 161, No. 1-3, (April 2009), pp. 188-192, DOI: 10.1016/j.mseb.2008.11.032

IntechOpen



Corrosion Resistance

Edited by Dr Shih

ISBN 978-953-51-0467-4

Hard cover, 472 pages

Publisher InTech

Published online 30, March, 2012

Published in print edition March, 2012

The book has covered the state-of-the-art technologies, development, and research progress of corrosion studies in a wide range of research and application fields. The authors have contributed their chapters on corrosion characterization and corrosion resistance. The applications of corrosion resistance materials will also bring great values to reader's work at different fields. In addition to traditional corrosion study, the book also contains chapters dealing with energy, fuel cell, daily life materials, corrosion study in green materials, and in semiconductor industry.

How to reference

In order to correctly reference this scholarly work, feel free to copy and paste the following:

Carlos Alberto Giudice (2012). Reinforcement Fibers in Zinc-Rich Nano Lithium Silicate Anticorrosive Coatings, Corrosion Resistance, Dr Shih (Ed.), ISBN: 978-953-51-0467-4, InTech, Available from:

<http://www.intechopen.com/books/corrosion-resistance/reinforcement-fibers-in-zinc-rich-nano-lithium-silicate-anticorrosive-coatings>

INTECH
open science | open minds

InTech Europe

University Campus STeP Ri
Slavka Krautzeka 83/A
51000 Rijeka, Croatia
Phone: +385 (51) 770 447
Fax: +385 (51) 686 166
www.intechopen.com

InTech China

Unit 405, Office Block, Hotel Equatorial Shanghai
No.65, Yan An Road (West), Shanghai, 200040, China
中国上海市延安西路65号上海国际贵都大饭店办公楼405单元
Phone: +86-21-62489820
Fax: +86-21-62489821

© 2012 The Author(s). Licensee IntechOpen. This is an open access article distributed under the terms of the [Creative Commons Attribution 3.0 License](#), which permits unrestricted use, distribution, and reproduction in any medium, provided the original work is properly cited.

IntechOpen

IntechOpen